Available online at www.sciencedirect.com
SCIENCE DIRECT
Trans. Nonferrous Met. Soc. China 17(2007) 1152−1157
Transactions of Nonferrous Metals Society of China
www.csu.edu.cn/ysxb/

Relationship between heat treatment and corrosion behaviour of Mg-3.0%Nd-0.4%Zr magnesium alloy

CHANG Jian-wei(常建卫), GUO Xing-wu(郭兴伍), FU Peng-huai(付彭怀),
PENG Li-ming(彭立明), DING Wen-jiang(丁文江)

National Engineering Research Center of Light Alloys Net Forming, School of Materials Science and Engineering, Shanghai Jiao Tong University, Shanghai 200030, China

Received 15 July 2007; accepted 10 September 2007

Abstract: The corrosion behaviour of Mg-3.0Nd-0.4Zr (NK30) magnesium alloy was investigated in as-cast (F), solution treated (T4) and peak-aged (T6) conditions in 5% NaCl solution by immersion tests and electrochemical measurements. The results of immersion test show that NK30 alloy exhibits better corrosion resistance in F condition than it does in the other two conditions due to the more compact corrosion film formed on alloy in F condition. The potentiodynamic polarization curves show that the overpotential of cathodic hydrogen evolution reaction on NK30-F is much higher than that on NK30-T4 and NK30-T6. The corrosion potentials of NK30 increase in the following order: F＜T4＜T6. The results of electrochemical impedance spectroscopy (EIS) also confirm that the corrosion film of NK30-F plays a more protective role than that of NK30-T4 and NK30-T6.

Key words: Mg-Nd-Zr alloy; corrosion behaviour; heat treatment; potentiodynamic polarization; electrochemical impedance spectroscopy

1 Introduction

Magnesium alloys have been widely used in the automotive, aircraft and aerospace industries and the interest in their application is continuously increasing. The most common Mg alloys are those alloyed with Al and Mn (e.g. AM50 and AM60) or with Al and Zn (e.g. AZ91), whose mechanical properties and corrosion behaviour are well established. Other Mg alloys, which have good castability, high strength at high temperature and good creep resistance, are obtained with rare earth(RE) elements (chiefly WE54 and WE43 alloys)[1].

Although the corrosion and electrochemical behaviours of Mg-Al or Mg-Mn alloy have been widely reported[2−7], data concerning Mg-RE alloys are scarce [8−11]. The later data seem to indicate that, in addition to favourable high temperature properties, certain Mg-RE alloys present good corrosion resistances. UNSWORTH and KING[8] have shown that WE54 alloy has a corrosion resistance comparable to that of A356 and A347 Al alloys for 28 d tests in sea water. In our previous study[9], the corrosion resistances of Mg-3.0Nd-0.2Zn-0.4Zr (NZ30K) alloy in three conditions (F, T4 and T6) were found to decrease in the following order: T4＞T6＞F. To date, there is no detailed study on the effect of heat treatment on corrosion behaviour of Mg-Nd-Zr ternary alloy. In this work, the relationship between heat treatment and corrosion behaviour of Mg-3.0Nd-0.4Zr (NK30) ternary alloy was investigated.

2 Experimental

The preparation of NK30 was similar to that of NZ30K in our previous study[9]. NK30 alloy has a nominal composition as Nd 3.0%, Zr 0.4% and Mg balance. The solution treatment (T4) was performed at 540 ℃ for 10 h in argon atmosphere and followed by water quenching at 25 ℃. The solution treatment alloy was aged artificially (T6) in an oil bath at 200 ℃ for 16 h. The corrosion test involved 3 d of immersion in 5% NaCl solution at (25±2) ℃. The specimens were polished with grit 1000 SiC paper before immersion test. At the end of the corrosion test, the corrosion products were removed in a chromic acid solution (200 g/L CrO_3+10 g/L $AgNO_3$) at 25 ℃ for 7 min and the mass

Foundation item: Project(5133003C) supported by the Major State Basic Research Development Program of China
Corresponding author: CHANG Jian-wei; Tel: +86-21-62932508; E-mail: changjw@sjtu.edu.cn

loss was measured. The morphologies of the corroded surfaces and corrosion products after immersion test were observed with SEM and FE-SEM, respectively.

Electrochemical measurements were carried out using a PARSTAT 2273 electrochemical system in a corrosion cell containing 5% NaCl solution saturated with $Mg(OH)_2$ using a three-electrode configuration: saturated calomel electrode as a reference, a platinum electrode as counter and the sample as working electrode. Polarization scan and electrochemical impedance spectroscopy(EIS) measurements were carried out after stabilization of the open circuit potential for 1h. EIS measurement was conducted at open circuit potential. The amplitude of applied alter current signal was 10 mV, and the measured frequency range was from 100 mHz to 1 MHz.

3 Results and discussion

3.1 Microstructure

The microstructures of NK30 alloy in as-cast (F), T4 and T6 conditions are shown in Fig.1. The microstructure of F alloy is composed of magnesium matrix and eutectic compound of $Mg_{12}Nd$ (Fig.1(a)). These eutectic compounds dissolve into the matrix after solution treatment (Fig.1(b)). The microstructure of T6 alloy is similar to that in T4 condition due to the tiny particle of precipitates in NK30-T6, which can not be seen in SEM micrographs[12]. Similar to NZ30K alloy, NK30 alloy also has Zr-rich cores existing in the centre of most grains in T4 and T6 conditions (Figs.1(b) and (c)). The magnified image shows that the Zr-rich cores are composed of hexagonal particles (Fig.1(d)), which is different from that of NZ30K alloy. In T4 and T6 NZ30K alloy, the Zr-rich cores are composed of block-like, globular and rob-like particles [9].

3.2 Immersion test

3.2.1 Corrosion of NK30 alloy

The corrosion rates of NK30 alloy after immersion in 5% NaCl solution for 3 d are shown in Fig.2. It can be seen that the corrosion resistances of NK30 in three conditions decrease in the following order: F＞T4＞T6. The corrosion rate of NK30 alloy under F condition is only 44% of that for NK30-T4 or 21% of that for NK30-T6.

In addition to the difference in corrosion rate, NK30 alloy exhibits different corrosion morphologies in three conditions. It can be seen from Fig.3 that the entire surface of NK30-F is covered with a compact yellowish corrosion film, while localized corrosion occurs on the surface of NK30-T4 and NK30-T6 alloy. Localized corrosion pits are covered with loose and white corrosion products. The area of localized corrosion on NK30-T6 is much larger than that on NK30-T4, and the corrosion of NK30-T6 is more severe than that of NK30-T4. The surface feature of the corroded specimens is in good agreement with the corrosion rates of Fig.2.

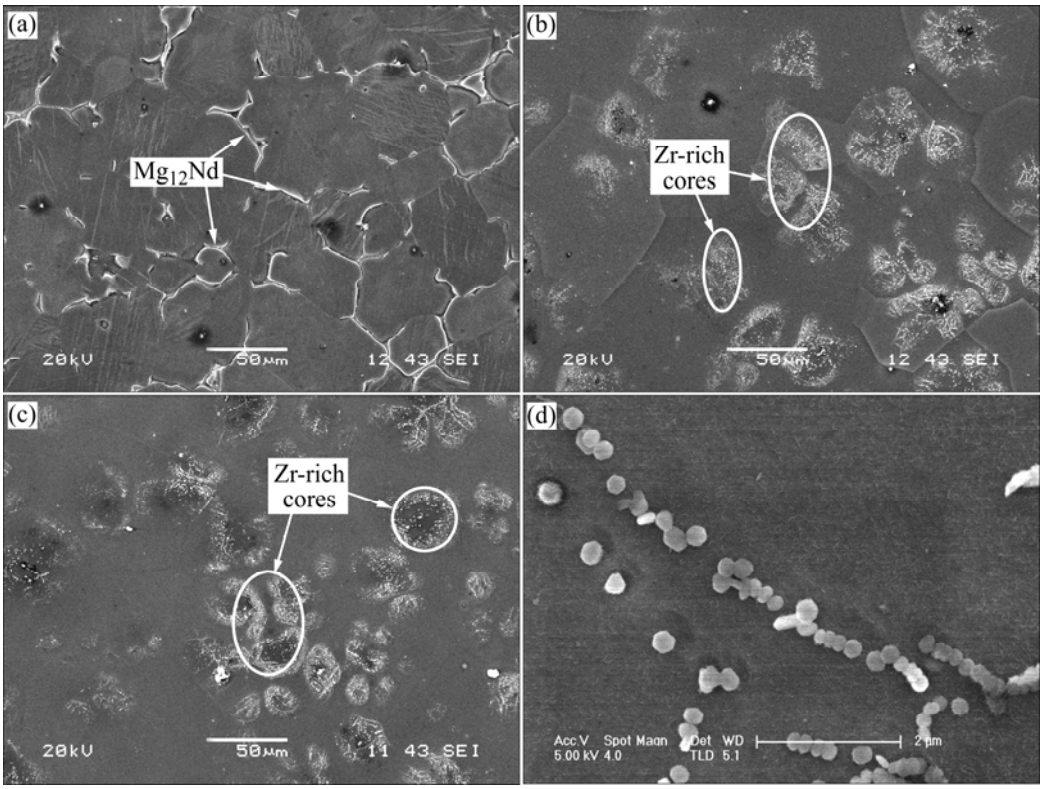

Fig.1 Scanning electron micrographs of NK30 alloy: (a) F; (b) T4; (c) T6; (d) Magnified image of Zr-rich cores in Fig.1(b)

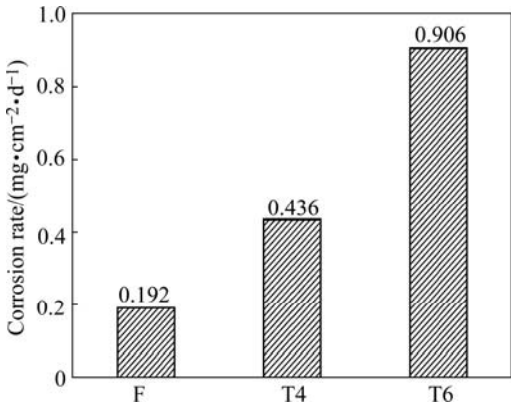

Fig.2 Corrosion rate of NK30 alloy after immersion in 5% NaCl solution for 3 d

Fig.3 Photographs of NK30 alloy after immersion in 5% NaCl solution for 3 d: (a) F; (b) T4; (c) T6

Fig.4 shows SEM morphologies of the corroded surface of NK30 alloy in three conditions after immersion in 5% NaCl solution for 3 d and removal of the corrosion products. It is clear that the corrosion initiates from the adjacent area of $Mg_{12}Nd$ compounds in NK30-F, but the corrosion is not severe (Fig.4(a)). Fig.5(a) also shows that no distinct corrosion pits exist on the surface of NK30-F, and the corrosion is more uniform. In NK30-T4 and NK30-T6 alloy, the corrosion initiates in the form of pits at several locations and then spreads over the surface in a filiform corrosion fashion (Figs.4(b) and (c)). Cross sections of the corroded areas indicate that corrosion attacks Zr-lack regions preferentially (Figs.5(b) and (c)), and Zr-rich cores have higher corrosion resistance than Zr-lack regions. The localized attack invades Zr-lack regions and leads to severe corrosion in these regions, while Zr-rich cores remain unaffected. After removal of the corrosion

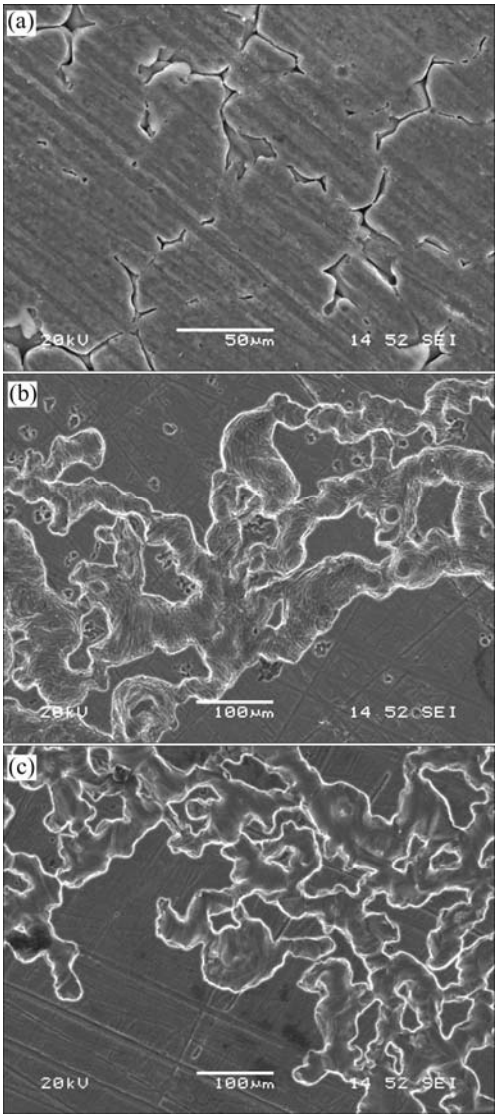

Fig.4 Scanning electron micrographs of corroded surfaces for NK30 alloy after immersion in 5% NaCl solution for 3 d and removal of corrosion products: (a) F; (b) T4; (c) T6

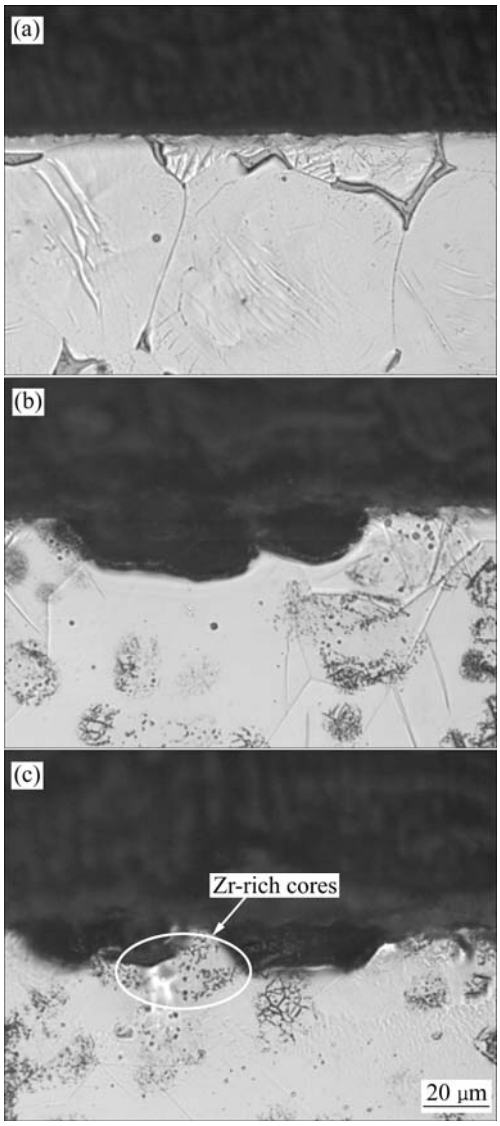

Fig.5 Typical optical micrographs of cross-sectional part adjacent to corroded surfaces for NK30 alloy after immersion in 5% NaCl solution for 3 d and removal of corrosion products: (a) F; (b) T4; (c) T6

products, NK30-T4 and MK30-T6 alloys show filiform-corrosion fashion (Figs.4(b) and (c)).

3.2.2 Corrosion products

At the end of the immersion test, the specimen surface was covered with a yellowish film of corrosion products. Fig.6 shows the FE-SEM morphologies of the corrosion products formed on NK30 alloy in different conditions after the immersion test. The corrosion product of NK30 alloy in three conditions is composed of voluminous tiny erect flakes. These flakes are aligned perpendicularly to the alloy surface. The thickness of the flakes of the corrosion product on NK30-T4 is much thinner than that on NK30-F. From the surface morphologies (Figs.6(a) and (b)) and cross sectional images (Figs.6(a′) and (b′)), it can be seen that the corrosion film on NK30-F is more compact than that on NK30-T4, and the amount of porosity in the corrosion film on NK30-F is lower than that on NK30-T4. Fig.6(c) shows that corrosion pits exist in NK30-T6. The results of XRD show that the corrosion product of NK30 is mainly $Mg(OH)_2$. The cross sectional images of the corrosion film in Figs.6(a′) and (b′) also show that the corrosion film presents two-layered structure (the outer layer and the transition layer). The outer layer is composed of erect flakes. An obvious transition layer exists between the outer layer and the substrate, but the transition layer is much thinner than the outer layer.

3.3 Electrochemical measurement

Fig.7 presents the potentiodynamic polarization curves (Fig.7(a)) and electrochemical impedance spectroscopy(EIS) results (Fig.7(b)) for the specimens after preliminary immersion for 1h in 5% NaCl solution saturated with $Mg(OH)_2$. Generally, the cathodic polarization curves are assumed to represent the cathodic hydrogen evolution through water, while the anodic ones represent the dissolution of magnesium. After 1 h immersion, the corrosion potential of NK30 alloy in three conditions increases in the following order: F＜T4 ＜T6.

The cathodic parts of the curves in Fig.7(a) indicate that the cathodic polarization current density of hydrogen evolution on NK30-F is much lower than that on NK30-T4 and NK30-T6 specimens. The polarization curve of NK30-T4 coincides with that of NK30-T6 in cathodic region. That is to say, the overpotential of the cathodic hydrogen evolution reaction on NK30-F is higher than that on NK30-T4 and NK30-T6. This reveals that the cathodic reaction is more difficult kinetically on the as-cast specimen than on the other two.

Fig.7(a) also shows the differences among the anodic curves of the specimens. The anodic portion of NK30-F is characterized by a clear current plateau, in which the current density increases very slowly over a narrow potential range followed by a rapid rate of increase with increasing potential, while no clear current plateau in the anodic portion of NK30-T4 and NK30-T6 is observed. The presence of the current plateau in the curve of NK30-F is due to the more protective film formed on NK30-F than those on NK30-T4 and NK30-T6 (Fig.6). After breaking down potential(E_{bd}) of NK30-F, the difference among the anodic curves of NK30 alloy under three conditions is not so significant as that in the cathodic curves. This indicates that the influence of heat treatment on the magnesium dissolution reaction in the corroding area is not so significant as its effect on the rate of cathodic hydrogen evolution.

The Nyquist plots of NK30 alloy under three conditions after immersion in 5% NaCl solution saturated with $Mg(OH)_2$ for 1h are presented in Fig.7(b).

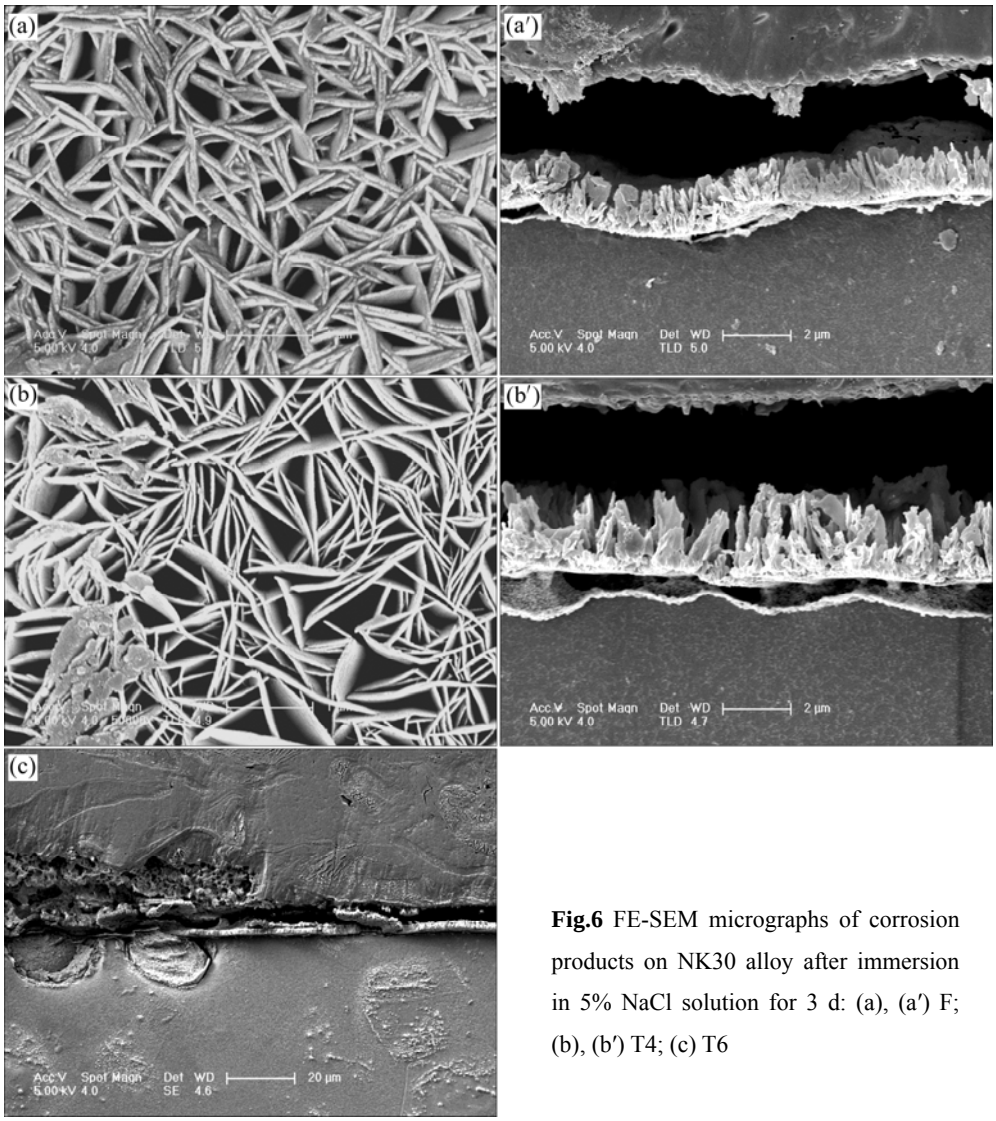

Fig.6 FE-SEM micrographs of corrosion products on NK30 alloy after immersion in 5% NaCl solution for 3 d: (a), (a′) F; (b), (b′) T4; (c) T6

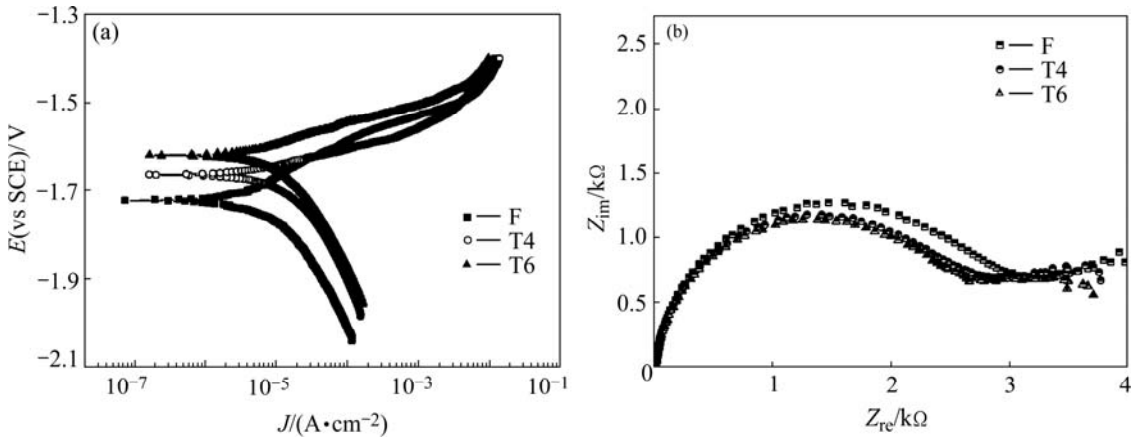

Fig.7 Electrochemical results of NK30 alloy after immersion in 5% NaCl solution saturated with $Mg(OH)_2$ for 1 h: (a) Polarization curves; (b) Nyquist curves

Their Nyquist plots are characterized by two capacitive loops, one for the high and medium frequencies, and the other for the low frequency, but the low frequency loop is depressed to some degree. The EIS spectra of NK30 alloy in three conditions are similar except for the difference in the diameter of the loops. This means that

the corrosion mechanisms of the alloy in three conditions are the same, but the their corrosion rates are different.

Referring to the previous studies[13], the high frequency loop appears to be ascribed to both charge transfer process and the film of corrosion products formed. The medium-frequency capacitive loop is ascribed to the relaxation of mass transport in the solid phase and disappears at long immersion time. The inductive loop at low frequency is due to the relaxation process of adsorbed species, such as $Mg(OH)^{+}_{ads}$, on the electrode surface. BRETT et al[14] have found that the pit formation leads to the inductive loop in the impedance spectra. In this study, the disappearance of the low frequency inductive loop shows that NK30 alloy has higher resistance of pitting corrosion. It can also be seen from Fig.7(b) that the dimension of high frequency capacitive loop of NK30 alloy in three conditions increases in the following order: F＞T4＞T6. This is in good agreement with the corrosion resistance of Fig.2. The good correlation between the high frequency loop and the corrosion resistance of NK30 alloy in three conditions in this study can be used as evidence to support the conclusion that the resistance associated with high frequency loop can be used to determine magnesium alloy corrosion rate[15].

4 Conclusions

1) Heat treatment influences the corrosion rate of NK30 alloy. The corrosion resistance of NK30 alloy in three conditions (F, T4 and T6) decreases in the following order: F＞T4＞T6.

2) The corrosion product of NK30-F is more compact than that of NK30-T4 and NK30-T6.

3) The potentiodynamic curves show that the overpotential of cathodic hydrogen evolution reaction on NK30-F is much higher than that on NK30-T4 and NK30-T6. The results of EIS also confirm that NK30-F alloy has the highest corrosion resistance in the three conditions.

References

[1] ZUCCHI F, GRASSI V, FRIGNANI A, MONTICELLI C, TRABANELLI G. Electrochemical behaviour of a magnesium alloy containing rare earth elements [J]. J Appl Electrochem, 2006, 36: 195−204.

[2] AMBAT R, AUNG N N, ZHOU, W. Evaluation of microstructural effects on corrosion behaviour of AZ91D magnesium alloy [J]. Corros Sci, 2000, 42: 1433−1455.

[3] SONG G L. Recent progress in corrosion and protection of magnesium alloys [J]. Adv Eng Mater, 2005, 7(7): 563−586.

[4] AMBAT R, AUNG N N, ZHOU W. Studies on the influence of chloride ion and pH on the corrosion and electrochemical behaviour of AZ91D alloy [J]. J Appl Electrochem, 2000, 30: 865−874.

[5] LI Y, ZHANG T, WANG F H. Effect of microcrystallization on corrosion resistance of AZ91D alloy [J]. Electrochim Acta, 2006, 51: 2845−2850.

[6] CHEN J, WANG J Q, HAN E H, DONG J H, KE W. AC impedance spectroscopy study of the corrosion behavior of an AZ91 magnesium alloy in 0.1 M sodium sulfate solution [J]. Electrochim Acta, 2007, 52: 3299−3309.

[7] HARA N, KOBAYASHI Y, KAGAYA D, AKAO N. Formation and breakdown of surface films on magnesium and its alloys in aqueous solutions [J]. Corros Sci, 2007, 49: 166−175.

[8] UNSWORTH W, KING J F. Magnesium technology [M]. London: The Institute of Metals, 1987: 25.

[9] CHANG J W, GUO X W, FU P H, PENG L M, DING W, J. Effect of heat treatment on corrosion and electrochemical behaviour of Mg-3Nd-0.2Zn-0.4Zr (wt.%) alloy [J]. Electrochim Acta, 2007, 52: 3160− 3167.

[10] ZUCCHI F, GRASSI A, FRIGNANI C. Electrochemical behaviour of a magnesium alloy containing rare earth elements [J]. J Appl Electrochem, 2006, 36: 195−204.

[11] GUO X W, CHANG J W, HE S M, DING W J, WAND X. Investigation of corrosion behaviors of Mg-6Gd-3Y-0.4Zr alloy in aqueous solutions [J]. Electrochim Acta, 2007, 52: 2570−2579.

[12] WILSON R, BETTLES C J, MUDDLE B C, Nie J F. Precipitation hardening in Mg-3wt%Nd(-Zn) casting alloys [J]. Mater Sci Forum, 2003, 419/412: 267−272.

[13] BARIL G, PEBERE N. The corrosion of pure magnesium in aerated and deaerated sodium sulphate solutions [J]. Corros Sci, 2001, 43: 471−484.

[14] BRETT C M A, DIAS L, TRINDADE, B, FISCHER R, MIES S. Characterisation by EIS of ternary Mg alloys synthesized by mechanical alloying [J]. Electrochim Acta, 2006, 51: 1752−1760.

[15] PEBERE N, RIERA C, DABOSI F. Investigation of magnesium corrosion in aerated sodium sulfate solution by electrochemical impedance spectroscopy [J]. Electrochim Acta, 1990, 35: 555−561.

(Edited by LI Xiang-qun)